Spin susceptibility of Andreev bound states

B. M. Rosemeyer and Anton B. Vorontsov

Spin susceptibility of Andreev bound states

B. M. Rosemeyer, Anton B. Vorontsov

Department of Physics, Montana State University, Montana 59717, USA

(Dated: September 6, 2016)

We calculate electronic spin susceptibility and spin-lattice relaxation rate in singlet superconductor near a pairbreaking surface, or in a domain wall of the order parameter. We directly link presence of high-density Andreev bound states in the inhomogeneous region, combined with coherence factors, to enhancement of the susceptibility above the normal state's value for certain $\mathbf{q}$ vectors. Beside the dominant peak at ferromagnetic vector $q = 0$, we find significant enhancement of antiferromagnetic correlations at vectors $q \lesssim 2k_f$, with $\mathbf{q}$ *along* the domain wall in S-wave superconductor, and *across* domain wall in D-wave (nodes along the wall). These features are destroyed by applying moderate Zeeman field that splits the zero-energy peak. We solve Bogoliubov-de Gennes equations in momentum space and discuss deviation of our results from the lattice models investigated previously. Large enhancement of the spin-lattice relaxation rate T_1^{-1} at the domain wall provides clear signature of the quasiparticle bound states, and is in good agreement with recent experiment in organic superconductor κ-(BEDT-TTF)$_2$Cu(NCS)$_2$.

I. INTRODUCTION

Soon after formulation of the BCS theory[1] Fulde, Ferrel[2] and Larkin, Ovchinnikov[3] (FFLO) pointed out that nonuniform superconducting states play an important role in strong magnetic fields or in magnetically-active materials. The most characteristic feature of nonuniform superconductors are distinct quasiparticle states that lie inside the energy gap of the bulk phase. They appear at pairbreaking surfaces in unconventional superconductors,[4] in vortex cores,[5] heterostructures,[6] and recently they were connected to topological properties of the order parameter.[7,8] Generally known as Andreev bound states (ABS) they are localized, for example, near a surface of a superconductor and decay into the bulk within a few coherence lengths $\xi_c = \hbar v_f / 2\pi k_B T_c$. If the bound states are all concentrated at one energy, producing a strong peak in the density of states (DOS), they dramatically change properties of the surface layer.

One important question is how the bound states affect magnetic properties of a material, in particular electronic spin susceptibility χ and spin-lattice relaxation rate T_1^{-1}. For example, in triplet superfluid ^{3}He these observables may provide a way to probe surface Majorana states.[9,10] In singlet superconductors they may be used to manipulate magnetic properties of the surface layer, or help prove or disprove existence of FFLO phases. This last goal is particularly relevant for several materials. In heavy-fermion superconductor CeCoIn$_5$, can an FFLO phase be the origin of coexistence[11–13] of antiferromagnetism (AFM) and superconductivity? On the other hand, is recently observed[14] enhancement of relaxation rate T_1^{-1} in organic superconductor κ-(BEDT-TTF)$_2$Cu(NCS)$_2$, indeed explained by Andreev bound states at FFLO domain walls?

Previous investigations of how nonuniform FFLO order parameter (OP) structures influence magnetic properties used quasiclassical techniques, and real-space lattice models. The quasiclassical calculations[15,16] show about 10% enhancement of uniform magnetization in-side FFLO domains at high fields where the FFLO phase appears. However, this technique cannot say anything about antiferromagnetic correlations with ordering vectors beyond $q \approx 1/\xi_c$. Several two-dimensional lattice Hamiltonians have been solved via Bogoliubov-de Gennes (BdG) equations to investigate co-existence of AFM order and FFLO states.[17–20] This approach can treat modulations on the order of Fermi momentum $q \sim 2k_f$. It was found that incommensurate spin-density wave (SDW) order can be induced inside the FFLO phase.[17,18] Other calculations show that transverse and longitudinal susceptibilities are enhanced up to 20% in zero field.[19] The incommensurate part of antiferromagnetic vector $\mathbf{q}$ was found mostly to point along the FFLO planes (i.e. $\mathbf{q} \perp \mathbf{q}_{FFLO}$),[17,18] independent of whether the planes were oriented along nodes or antinodes of the $D_{x^2-y^2}$ order parameter. $\mathbf{q}$ across FFLO planes was not favored, except in the case of atomic-scale FFLO oscillations.[19,20] The spatially-averaged approach[19] has also only considered small-period modulations of the order parameter. In Ref. 18 appearance of AFM was correlated with presence of multiple FFLO domain walls, but no mechanism directly linking AFM and localized ABS was established.

The effects of the bound states have been investigated in vortex phases, near vortex cores. The localized states in cores and enhancement of local density of states (LDOS) were predicted[21] to produce faster relaxation time T_1 of electronic spins, which was later seen by spatially-resolved NMR in S-wave superconductor.[22] Bound states can result in enhancement of T_1^{-1} over the normal state value even in D-wave,[23] producing 'false Hebel-Slichter' peak below T_c. In Pauli-limited D-wave superconductors vortices can lead to SDW instability with $\mathbf{q} \parallel$nodes by increasing DOS for near-nodal directions.[24] Moreover, the core region of vortices often have enhanced SDW correlations[25–27] with $\mathbf{q}$ across the core, but again the role of the bound states for these correlations has not been explicitly shown.

To clarify the role of the Andreev bound states and manifestly connect them with magnetic properties, we

consider a prototypical non-uniform structure of Larkin-Ovchinnikov kind: a domain wall that separates semi-infinite regions of positive/negative amplitude of the order parameter, Fig. (1). Near the wall the density of states is strongly peaked for zero-energy excitations, arising as result of topological properties of Dirac-type equation.[7,8] We consider itinerant 2-D electrons with S- or D-wave pairing symmetry. For D-wave we orient the domain wall along gap nodes,[28] which also corresponds to a pairbreaking surface in a half-space problem. We solve the Bogoliubov-de Gennes equations in momentum space, which directly relates the Fermi surface properties, symmetry of the order parameter, and momentum dependence of the quasiparticle states to the observables. This approach also naturally connects to the quasiclassical theory.

We find that the bound states lead to increase in the transverse spin susceptibility of a superconductor which may lead to SDW ordering. The specific ordering wave vectors $\mathbf{q}$ connect 'hot spots' on the Fermi surface with large bound state weights determined by coherence factors, that depend on the symmetry of the order parameter. We find that generally S-wave symmetry favors AFM ordering vector along the domain wall, whereas inside D-wave nodally-oriented domain wall the ordering vector points across it. We also calculate relaxation rate T_1^{-1} for FFLO, that so far has been lacking. The bound states give large relaxation rate T_1^{-1} when quasiparticle transitions between bound states and continuum states can occur. We find that application of Zeeman field that splits the zero-energy states by $2\mu_B H$ generally reduces tendency toward AFM ordering inside the domain wall.

The remainder of this report is organized as follows. In section II we define our two-dimensional model Hamiltonian with a mean-field two-point order parameter $\Delta(\mathbf{x}, \mathbf{x}')$. We solve it via Bogoliubov-de Gennes equations and find quasiparticle spectrum and amplitudes in momentum space, which we use to calculate the electron susceptibility and spin-lattice relaxation rate. We employ a new numeric technique using a Fast Fourier Transform for all momenta near the Fermi surface, which is more suitable to calculating momentum dependent quantities. In section III we present results of the calculations, and we end in section IV with a discussion of the implications of our findings for recent experiments. Finally, we provide appendix with outline of the self-consistent method we are using.

II. MODEL

We work with the Hartree-Fock-Bogoliubov (HFB) mean-field Hamiltonian for a single band

$$\mathcal{H}_{HFB} = \frac{1}{2} \int d\mathbf{x} d\mathbf{x}' \quad \Psi^\dagger(\mathbf{x}) \, \mathcal{H}(\mathbf{x}, \mathbf{x}') \, \Psi(\mathbf{x}') \quad (1)$$

where we have defined the field operator $\Psi^\dagger(\mathbf{x}) = \left(\psi_\uparrow^\dagger(\mathbf{x}), \psi_\downarrow^\dagger(\mathbf{x}), \psi_\uparrow(\mathbf{x}), \psi_\downarrow(\mathbf{x}) \right)$, and $\mathcal{H}(\mathbf{x}, \mathbf{x}')$ is a 4×4 block
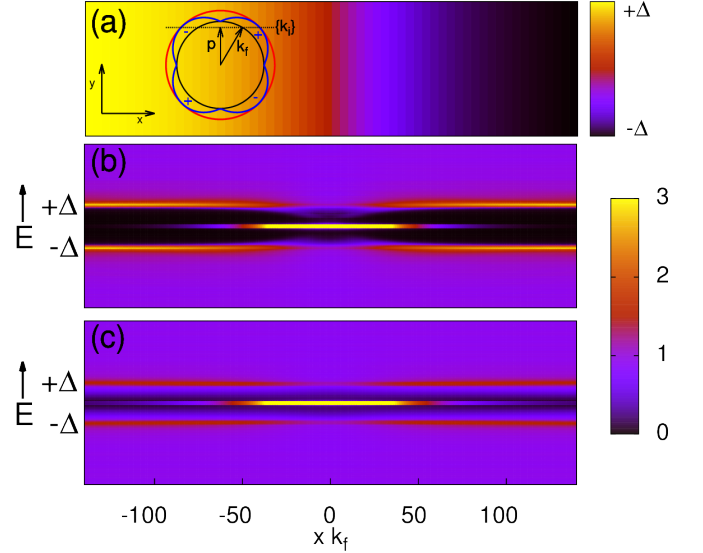

FIG. 1. (a) Domain wall $+\Delta \to -\Delta$ in x-direction with translational invariance along y. Inset shows relative orientation of the domain wall plane and internal symmetry of the order parameter, S (red) or D-wave (blue). (b) The normalized local density of states $N(\epsilon, x)/N_f$ for S-wave domain wall, and (c) the same for D-wave with nodes $\parallel x$. The zero-energy states appear at the domain wall. We use $\Delta_0 = 0.05\epsilon_f$ throughout the paper that results in $\xi_c k_f \sim 12$.

matrix

$$\mathcal{H}(\mathbf{x}, \mathbf{x}') = \begin{pmatrix} \hat{\mathcal{H}}_0 \, \delta(\mathbf{x} - \mathbf{x}') & \hat{\Delta}(\mathbf{x}, \mathbf{x}') \\ -\hat{\Delta}^*(\mathbf{x}, \mathbf{x}') & -\hat{\mathcal{H}}_0^* \, \delta(\mathbf{x} - \mathbf{x}') \end{pmatrix} . \quad (2)$$

$\hat{\mathcal{H}}_0 = \left[\frac{-\nabla^2}{2m^*} - \epsilon_f \right] \hat{1} - \mu_B H \sigma^z$ describes free electrons in a Zeeman field, m^* is the effective mass of the electron, ϵ_f is the Fermi energy, H is the applied magnetic field and μ_B is the Bohr magneton. $\sigma^{\alpha=\{x,y,z\}}$ are the Pauli matrices. The singlet superconducting pair potential is self-consistently defined as

$$\hat{\Delta}(\mathbf{x}, \mathbf{x}') = (i\sigma^y)\Delta(\mathbf{x}, \mathbf{x}') \quad (3)$$

$$\Delta(\mathbf{x}, \mathbf{x}') = V(\mathbf{x} - \mathbf{x}')\langle \psi_\beta(\mathbf{x}')\psi_\alpha(\mathbf{x})\rangle(i\sigma^y)_{\alpha\beta} \quad (4)$$

where summation over repeated spin indices is implied, and $\langle ... \rangle$ denotes ensemble average. $V(\mathbf{x} - \mathbf{x}')$ is the effective attractive interaction that leads to superconductivity, with the cut-off energy Λ.

Since we expect presence of degenerate zero-energy states we need to define Bogoliubov-Valatin canonical transformation with some care.[6] We take

$$\begin{bmatrix} \psi_\mu \\ \psi_\mu^\dagger \end{bmatrix} (\mathbf{x}) = \sum_{\mathbf{n}} U_{\mathbf{n},\mu\nu}^{(+)}(\mathbf{x}) \, \gamma_{\mathbf{n}\nu} + U_{\mathbf{n},\mu\nu}^{(-)}(\mathbf{x}) \, \gamma_{\mathbf{n}\nu}^\dagger , \quad (5)$$

where the state index $\mathbf{n}$ for inhomogeneous superconductor replaces momenum $\mathbf{k}$, used to label states in uniform superconductor. To treat the zero-energy states in the same way as finite-energy states, $\mathbf{n}$ labels all positive energy states, and *half* of zero-energy states, as we explain

below. The $U_{\mathbf{n}}^{(\pm)}(\mathbf{x})$ are two eigenvectors of the Hamiltonian (2) corresponding to positive and negative energy branches

$$\int d\mathbf{x}'\mathcal{H}(\mathbf{x},\mathbf{x}')U_{\mathbf{n}}^{(\pm)}(\mathbf{x}') = \pm\epsilon_{\mathbf{n}}U_{\mathbf{n}}^{(\pm)}(\mathbf{x}) \qquad (6)$$

Due to particle-hole symmetry of HFB Hamiltonian, for each $\mathbf{n}$ there is a pair of $\pm\epsilon_{\mathbf{n}}$ states, related to each other through

$$U_{\mathbf{n},\mu\nu}^{(+)}(\mathbf{x}) = \begin{bmatrix} \delta_{\mu\nu}\,u_{\mathbf{n}} \\ -i\sigma_{\mu\nu}^{y}v_{\mathbf{n}} \end{bmatrix} \quad , \quad \tilde{U}_{\mathbf{n},\mu\nu}^{(-)}(\mathbf{x}) = \begin{bmatrix} -i\sigma_{\mu\nu}^{y}v_{\mathbf{n}}^{*} \\ \delta_{\mu\nu}\,u_{\mathbf{n}}^{*} \end{bmatrix}$$

The non-zero energy states are naturally represented by $\gamma_{\mathbf{n}\mu}$ and $\gamma_{\mathbf{n}\mu}^{\dagger}$ terms in (5). However as a consequence of the particle-hole symmetry, the zero-energy states also come in pairs, and assignment of $\gamma_{0\mu}$ or $\gamma_{0\mu}^{\dagger}$ to them is somewhat arbitrary. To avoid double-counting of zero-energy states in (5), we take half of them and assign it to 'positive' solutions (γ, $U^{(+)}$) and the other half appear as 'negative' part ($\gamma^{\dagger}$, $U^{(-)}$). To find the positive energy states we solve Bogoliubov-de Gennes equations, and in case of singlet superconductivity they are spin-independent:

$$\epsilon_{\mathbf{n}}u_{\mathbf{n}}(\mathbf{x}) = \xi(-i\boldsymbol{\nabla})u_{\mathbf{n}}(\mathbf{x}) + \int d\mathbf{x}'\Delta(\mathbf{x},\mathbf{x}')v_{\mathbf{n}}(\mathbf{x}')$$
$$\epsilon_{\mathbf{n}}v_{\mathbf{n}}(\mathbf{x}) = -\xi(-i\boldsymbol{\nabla})^{*}v_{\mathbf{n}}(\mathbf{x}) + \int d\mathbf{x}'\Delta^{*}(\mathbf{x},\mathbf{x}')u_{\mathbf{n}}(\mathbf{x}') \qquad (7)$$

where $\xi(-i\boldsymbol{\nabla}) = (-i\boldsymbol{\nabla})^{2}/2m^{*} - \epsilon_{f}$. In Zeeman field The quasi-particle excitation energy is simply shifted to $\epsilon_{\mathbf{n}\mu} = \epsilon_{\mathbf{n}} - \mu_{B}H\,\sigma_{\mu\mu}^{z}$ and the full Hamiltonaian in diagonal form is $\mathcal{H}_{HFB} = E_{0} + \sum_{\mathbf{n}\mu}\epsilon_{\mathbf{n}\mu}\gamma_{\mathbf{n}\mu}^{\dagger}\gamma_{\mathbf{n}\mu}$. Finally, orthogonality of solutions with $\mathbf{n} \neq \mathbf{n}'$, and orthogonality of positive and negative solutions for the same $\mathbf{n}$ result in two normalization conditions:

$$\int d\mathbf{x}\,[u_{\mathbf{n}}(\mathbf{x})u_{\mathbf{n}'}^{*}(\mathbf{x}) + v_{\mathbf{n}}(\mathbf{x})v_{\mathbf{n}'}^{*}(\mathbf{x})] = \delta_{\mathbf{n}\mathbf{n}'} \qquad (8)$$

$$\int d\mathbf{x}\,[u_{\mathbf{n}}(\mathbf{x})v_{\mathbf{n}'}(\mathbf{x}) - v_{\mathbf{n}}(\mathbf{x})u_{\mathbf{n}'}(\mathbf{x})] = 0 \qquad (9)$$

For the domain wall, or stripes configuration, one has translational invariance along the wall ($\hat{y}$) with momentum quantum numbers $\{p\}$. In the transverse direction the wave function for given p is expanded into Fourier Series

$$u_{\mathbf{n}}(\mathbf{x}) = e^{ipy}\sum_{j=0}^{N-1}\tilde{u}_{\mathbf{n}}(k_{j})e^{ik_{j}x}\,,$$
$$v_{\mathbf{n}}(\mathbf{x}) = e^{ipy}\sum_{j=0}^{N-1}\tilde{v}_{\mathbf{n}}(k_{j})e^{ik_{j}x}\,. \qquad (10)$$

We employ a Fast Fourier Transform technique with

$$\frac{k_{j}}{k_{f}} = \begin{cases} 4\pi j/N, & j \leq N/2 \\ -4\pi(N-j)/N, & j > N/2 \end{cases}$$

and periodic boundary conditions at $k_{f}x = 0$ and $k_{f}x = N/2$ (k_{f} is the Fermi momentum). The reasons for beginning with a doubled Fourier domain $(-2\pi, 2\pi)$ is because the calculation of the relative momentum spin susceptibility will half the domain to $(-\pi, \pi]$ while doubling the spatial domain to $(-N/2, N/2)$. We use $N = 2^{12} = 4096$ momentum grid points.

For efficient numerics, we restrict our set of transverse momenta $\{k_{j}\}$ for each p to include only those whose normal excitation energy

$$\xi(p, k_{j}) = \frac{k_{j}^{2} + p^{2}}{2m^{*}} - \epsilon_{f}, \qquad (11)$$

is below an energy cut-off, $|\xi_{p,k_{j}}| \leq \Lambda$. All higher energy solutions to (7) are considered normal with $\Delta(\mathbf{x},\mathbf{x}') = 0$.

Furthermore, since we are interested in low-energy superconducting quasiparticles, we take a separable form of the pair potential, described by the amplitude that depends on the center of mass coordinate $\mathbf{R}$, and the internal symmetry profile $g(\mathbf{r})$ that depends on the relative coordinate $\mathbf{r}$,

$$\mathbf{R} = \frac{\mathbf{x} + \mathbf{x}'}{2} \qquad \mathbf{r} = \mathbf{x} - \mathbf{x}'\,,$$
$$\Delta(\mathbf{x},\mathbf{x}') = \Delta(\mathbf{R},\mathbf{r}) = \Delta(\mathbf{R})\left[\int\frac{d\mathbf{L}}{(2\pi)^{2}}\,g_{\hat{L}}e^{i\mathbf{L}\cdot\mathbf{r}}\right]\,, \qquad (12)$$

where $\mathbf{L}$ is the relative momentum in a Cooper pair. We consider S-wave and D-wave pairing states:

$$S-wave: \quad g_{\hat{L}} = 1$$
$$D-wave: \quad g_{\hat{L}} = \sin(2\theta_{\hat{L}}) \quad \text{or} \quad g_{\hat{L}} = \cos(2\theta_{\hat{L}}) \qquad (13)$$

where $\theta_{\hat{L}}$ is the angle of $\mathbf{L}$ measured from the x-axis. The profile of the order parameter across the domain wall depends only on coordinate x, $\Delta(\mathbf{R}) = \Delta(x)$.

Using equations (10) for the amplitudes, (7) becomes a matrix eigenvalue equation for $\epsilon_{\mathbf{n}}$, where the $2N$ Fourier coefficients, $\tilde{\mathcal{U}}_{\mathbf{n}}^{T} = (\tilde{u}_{\mathbf{n}}(k_{0}), \tilde{u}_{\mathbf{n}}(k_{1})...\tilde{u}_{\mathbf{n}}(k_{N-1}), \tilde{v}_{\mathbf{n}}(k_{0}), \tilde{v}_{\mathbf{n}}(k_{1})...\tilde{v}_{\mathbf{n}}(k_{N-1}))$ form the eigenvector for each longitudinal momentum p,

$$\epsilon_{\mathbf{n}}\tilde{\mathcal{U}}_{\mathbf{n}} = \begin{pmatrix} \overset{\leftrightarrow}{\xi}_{p} & \overset{\leftrightarrow}{\Delta}_{p} \\ \overset{\leftrightarrow}{\Delta}_{p}^{*} & -\overset{\leftrightarrow}{\xi}_{p} \end{pmatrix}\tilde{\mathcal{U}}_{\mathbf{n}} \qquad (14)$$

where $\overset{\leftrightarrow}{\xi}_{p}$ and $\overset{\leftrightarrow}{\Delta}_{p}$ are $N \times N$ matrices with $(i,j)th$ entries

$$\overset{\leftrightarrow}{\xi}_{p}(i,j) = \left(\frac{k_{i}^{2} + p^{2}}{2m_{e}} - \epsilon_{f}\right)\delta_{ij} \qquad (15)$$

$$\overset{\leftrightarrow}{\Delta}_{p}(i,j) = g_{\hat{L}_{ij}}\int dx\,\Delta(x)e^{-i(k_{i}-k_{j})x} \qquad (16)$$

and $\mathbf{L}_{ij} = \frac{k_{i}+k_{j}}{2}\hat{x} + p\hat{y}$. Solving (14) we obtain $2N$ eigenstates, out of which N have positive (and zero) energies, and N has mirror negative (and zero) energies. We arrange solutions from negative to positive energies, and the quantum number $\mathbf{n} = (p, n)$ labels top N energy

states. This guarantees that it goes over all positive $\epsilon_{\mathbf{n}}$ and half of zero-energy solutions.

We consider a system where we apply a uniform static field $\mathbf{H}_0$, and consider a magnetic response to a small perturbation of the magnetic field $\delta\mathbf{H}(\mathbf{x},\omega) = \int dt e^{i\omega t}\delta\mathbf{H}(\mathbf{x},t)\Theta(t)$, where $\Theta(t)$ is the Heaviside step function. Up to first order in perturbation the electron magnetization is

$$M_\alpha(\mathbf{x},\omega) = M_{0,\alpha} + \delta M_\alpha(\mathbf{x},\omega) \quad (17)$$

$$\delta M_\alpha(\mathbf{x},\omega) = \int d\mathbf{x}' \, \chi_{\alpha\beta}(\mathbf{x},\mathbf{x}',\omega)\,\delta H_\beta(\mathbf{x}',\omega) \quad (18)$$

where $\mathbf{M}_0$ is the magnetization in the superconducting state due to the uniform field $\mathbf{H}_0$. The bare susceptibility $\chi_{\alpha\beta}(\mathbf{x},\mathbf{x}',\omega)$ is given by the Kubo formula[29]

$$\chi_{\alpha\beta}(\mathbf{x},\mathbf{x}',\omega) = i\mu_B^2 \int dt \, e^{i\omega t} \langle [S_\alpha(\mathbf{x},t), S_\beta(\mathbf{x}',0)]\Theta(t)\rangle \quad (19)$$

where $\mathbf{S}(\mathbf{x},t) = \sum_{\mu\nu}\psi_\mu^\dagger(\mathbf{x},t)\boldsymbol{\sigma}_{\mu\nu}\psi_\nu(\mathbf{x},t)$ is the spin operator and $\omega = \omega' + i\omega''$ is assumed to have a small imaginary part for convergence of the time integration ($\omega'' \ll \Delta_0$, Δ_0 is the gap energy at $T=0, H=0$).

Without effects that introduce spin-orbit coupling, the isotropy of spin space is broken only by $\mathbf{H}_0$. Then the susceptibility tensor is diagonal in longitudinal($\delta\mathbf{H} \parallel \mathbf{H}_0$)-transverse($\delta\mathbf{H} \perp \mathbf{H}_0$) space. We are mostly interested in cases when the induced or spontaneous magnetization is orthogonal to uniform state $\delta\mathbf{M}(\mathbf{q},\omega) \perp \mathbf{M}_0$. Using the Bogoliubov-Valatin transformation, the normalized transverse susceptibility is

$$\chi_\perp(\mathbf{x},\mathbf{x}',\omega) = \frac{2\mu_B^2}{\chi_0} \sum_{\mathbf{nn}'\mu} \Big[A_{\mathbf{nn}'}(\mathbf{x})A_{\mathbf{nn}'}^*(\mathbf{x}')\Pi_{\mathbf{n}\mu;\mathbf{n}'\bar\mu}^+(\omega)$$
$$+ \frac{1}{2}C_{\mathbf{nn}'}^*(\mathbf{x})C_{\mathbf{nn}'}(\mathbf{x}')\Pi_{\mathbf{n}\mu;\mathbf{n}'\mu}^-(\omega)$$
$$+ \frac{1}{2}C_{\mathbf{nn}'}(\mathbf{x})C_{\mathbf{nn}'}^*(\mathbf{x}')\Pi_{\mathbf{n}\mu;\mathbf{n}'\mu}^-(-\omega)\Big] \quad (20)$$

Here $\bar\mu$ denotes spin state opposite to μ,

$$\Pi_{\mathbf{n}\mu;\mathbf{n}'\nu}^\pm(\omega) = \frac{f(\epsilon_{\mathbf{n}\mu}) - f(\pm\epsilon_{\mathbf{n}'\nu})}{\omega + \epsilon_{\mathbf{n}\mu} \mp \epsilon_{\mathbf{n}'\nu}}, \quad (21)$$

$f(\epsilon)$ is the Fermi distribution function, and $\chi_0 = 2\mu_B^2 N_f$ is the Pauli susceptibility in the normal state, N_f is the DOS at the Fermi energy per spin projection. For energies close to zero, or much less than temperature spread of the Fermi-Dirac distribution,

$$\Pi_{\mathbf{n}\mu;\mathbf{n}'\nu}^\pm(\omega) \approx \frac{\partial f}{\partial\epsilon}\frac{\epsilon_{\mathbf{n}\mu} \mp \epsilon_{\mathbf{n}'\nu}}{\omega + \epsilon_{\mathbf{n}\mu} \mp \epsilon_{\mathbf{n}'\nu}} = \frac{\epsilon_{\mathbf{n}\mu} \mp \epsilon_{\mathbf{n}'\nu}}{4T(\omega + \epsilon_{\mathbf{n}\mu} \mp \epsilon_{\mathbf{n}'\nu})}.$$

Combinations of quasiparticle amplitudes

$$A_{\mathbf{nn}'}(\mathbf{x}) = u_{\mathbf{n}}^*(\mathbf{x})u_{\mathbf{n}'}(\mathbf{x}) + v_{\mathbf{n}}^*(\mathbf{x})v_{\mathbf{n}'}(\mathbf{x}) \quad (22)$$

$$C_{\mathbf{nn}'}(\mathbf{x}) = u_{\mathbf{n}}(\mathbf{x})v_{\mathbf{n}'}(\mathbf{x}) - v_{\mathbf{n}}(\mathbf{x})u_{\mathbf{n}'}(\mathbf{x}) \quad (23)$$

are the coherence factors (of type II corresponding to perturbations that break time reversal symmetry[30]). They determine the spatial dependence of susceptibility, while the remaining terms are functions of energy and temperature.

We note that the combinations $A_{\mathbf{nn}'}(\mathbf{x})A_{\mathbf{nn}'}^*(\mathbf{x}')$ and $C_{\mathbf{nn}'}^*(\mathbf{x})C_{\mathbf{nn}'}(\mathbf{x}')$ in (20) under coordinate exchange $\mathbf{x} \leftrightarrow \mathbf{x}'$ ($\mathbf{r} \leftrightarrow -\mathbf{r}$) become complex conjugated. This symmetry guarantees that local susceptibility at wave vector $\mathbf{q}$

$$\chi(\mathbf{R},\mathbf{q},\omega) = \int d\mathbf{r}\, e^{-i\mathbf{q}\cdot\mathbf{r}}\chi(\mathbf{R},\mathbf{r},\omega) = \chi' + i\chi'', \quad (24)$$

has real part χ' that depends only on the *real* part of $\Pi_{\mathbf{n}\mu;\mathbf{n}'\nu}^\pm$, and the imaginary part χ'' has contributions only from the *imaginary* part of $\Pi_{\mathbf{n}\mu;\mathbf{n}'\nu}^\pm$.

Lastly, we find the spin-lattice relaxation rate T_1^{-1} due to the hyperfine interaction between nuclear spins $\mathbf{I}(\mathbf{x}_s)$ and electron spins $\mathbf{S}(\mathbf{x})$

$$\mathcal{H}_{hf} = \int d\mathbf{x}d\mathbf{x}_s\, \mathbf{I}(\mathbf{x}_s) \cdot \mathcal{A}(\mathbf{x}_s - \mathbf{x}) \cdot \mathbf{S}(\mathbf{x}) \quad (25)$$

$\mathcal{A}(\mathbf{r})$ is the 3×3 hyperfine matrix. For transitions between spin $1/2$ nuclear states which are well below the thermal energy ($\epsilon_i - \epsilon_f = \omega << T$), and if $\mathcal{A}(\mathbf{r})$ is strongly peaked near $\mathbf{r} = 0$, the spin-lattice relaxation rate due to $\mathcal{A}_\perp$ is found using first order perturbation theory,[31]

$$T_1^{-1}(\mathbf{R},\omega) = 2T \lim_{\omega\to 0} \sum_{\mathbf{q}} |\mathcal{A}_\perp(\mathbf{q})|^2 \frac{\chi_\perp''(\mathbf{R},\mathbf{q},\omega)}{\omega} \quad (26)$$

The details of $\mathcal{A}_\perp(\mathbf{q})$ depend on the interactions of the spin fields, however in an effort to focus on the DW effects we consider only the simplest isotropic coupling, $\mathcal{A}_\perp(\mathbf{q}) = A_0$.

III. RESULTS AND ANALYSIS

We first find the profile of the order parameter for the domain wall configuration. The details of the self-consistent calculation are presented in appendix and the general solution is shown in Fig. 1(a). The local density of states for spin projection μ is $N_\mu(\epsilon,\mathbf{x}) = -(1/\pi)Im[G_\mu^R(\epsilon,\mathbf{x})]$ where $G_\mu^R(\epsilon,\mathbf{x})$ is the retarded Greens function,

$$G_\mu^R(\epsilon,\mathbf{x}) = -i\int_0^\infty dt\, e^{i(\epsilon+i0)t}\langle[\psi_\mu(\mathbf{x},t)\,,\,\psi_\mu^\dagger(\mathbf{x},0)]_+\rangle$$

$$= \sum_{\mathbf{n}} \left[\frac{|u_{\mathbf{n}}(\mathbf{x})|^2}{\epsilon - \epsilon_{\mathbf{n}\mu} + i0} + \frac{|v_{\mathbf{n}}(\mathbf{x})|^2}{\epsilon + \epsilon_{\mathbf{n}\bar\mu} + i0}\right]$$

average $\langle\ldots\rangle$ is over the ground state of the superconductor. LDOS is presented in figure 1(b,c) for S- and D-wave pairings. The large zero-energy peak appears at the domain wall, confined on the scale of $10\xi_c$ ($\xi_c = v_f/2\pi T_c$).

In magnetic field the spectrum is Zeeman-shifted and the bound states appear at energies $\pm\mu_B H_0$ for up/down spins. We perform calculations by introducing a cutoff in energy $\Lambda = 5\Delta_0$, above which we treat states as if in normal metal, and checked that doubling of Λ does not change our results. We set zero-temperature gap in terms of Fermi energy $\Delta_0 = 0.05\epsilon_f$, which results in coherence lengths $\xi_c^s = 11.2/k_f$ (S-wave) and $\xi_c^d = 13.6/k_f$ (D-wave). The cutoff provides a rough separation of low and high energy scales, and one can break the double sum over $\mathbf{n}$ and $\mathbf{n}'$ in susceptibility (20) into three contributions

I	$\epsilon_{\mathbf{n}} < \Lambda, \ \epsilon_{\mathbf{n}'} < \Lambda$		low-ϵ
II	$\epsilon_{\mathbf{n}} < \Lambda, \ \epsilon_{\mathbf{n}'} > \Lambda;$	$(\mathbf{n} \leftrightarrow \mathbf{n}')$	mixed-ϵ
III	$\epsilon_{\mathbf{n}} > \Lambda, \ \epsilon_{\mathbf{n}'} > \Lambda$		high-ϵ

A. Real Susceptibility

We calculate the deviation of local susceptibility in non-uniform superconductor from the known normal state value

$$\delta\chi(x, \mathbf{q}, \omega) = \chi(x, \mathbf{q}, \omega) - \chi_N(|\mathbf{q}|, \omega), \qquad (27)$$

which means cancellation of high-energy part III in (20). Mixed terms II are only slightly affected by superconductivity and we find their contribution to $\delta\chi/\chi_N$ to be $< 1\%$ for all relevant $\mathbf{q}$ vectors. Thus, to reduce numerical cost and to obtain high-$\mathbf{q}$ resolution figures, we compute only the dominant low-energy region terms that we denote $\delta\chi_I$.

In figure 2 we show zero-field results for local static susceptibility ($\omega = 0$) in the middle of the domain wall ($x = 0$) as a function of the ordering vector $\mathbf{q}$. The susceptibility is clearly increased for uniform magnetization $q \approx 0$, due to large density of bound states at zero energy. There are also several regions of non-zero $q \sim k_f$, for which $\chi_\perp$ is significantly enhanced over the normal state value, showing tendency towards antiferromagnetic ordering. In S-wave superconductor, Fig. 2(left), the direction of such $\mathbf{q}$ vectors is along the y-axis, i.e. pointing along the domain wall.

When the domain wall is along nodes of D-wave order parameter, Fig. 2(middle), the ordering vector $\mathbf{q}$ showing enhanced susceptibility is along the diagonal directions for small $q_x/k_f \approx \pm q_y/k_f$, and for $(q_x, q_y) \sim (1.75k_f, 0)$ that shows about 15% enhancement over χ_0. The latter means that if antiferromagnetic SDW order is induced by the non-uniform superconductivity, its modulation vector will be normal to the order parameter domain wall, or normal to the pairbreaking surface if we consider semi-infinite superconductor. For the domain wall in antinodal orientation, Fig. 2(right), enhancement appears at multiple $\mathbf{q}$s, including $\hat{y}$ direction similar to S-wave, and diagonal $\mathbf{q} \sim (1.25, 1)k_f$.

We associate these regions of enhancement exclusively with correlations between bound states. Overall, one expects the biggest change in static $\omega = 0$ susceptibility from terms in (20) that have vanishing denominators of (21) i.e. $\epsilon_{\mathbf{n}\mu} \pm \epsilon_{\mathbf{n}'\mu'} \to 0$. Thus, the $(\mathbf{n}\mu; \mathbf{n}'\nu)$ term which connects two bound states with zero energies should give a large contribution. The magnitude of this contribution, however, is also determined by the phase space, or the weight of zero-energy state, and spatial dependence of the coherence factors. This determines the direction of $\mathbf{q}$ for maximally enhanced $\delta\chi$.

To understand the role of coherence factors one can use the Andreev approximation to estimate the BdG $u_{\mathbf{n}}, v_{\mathbf{n}}$ amplitudes. The state index can be written as $\mathbf{n} = (\hat{k}, n)$, where $\hat{k}$ is the unit vector that defines a quasiclassical trajectory, and n labels states along this trajectory:

$$u_{\mathbf{n}}(\mathbf{x}) = u_{\hat{k}, n}(\mathbf{x})e^{ip_f \hat{k}\cdot\mathbf{x}}, \qquad v_{\mathbf{n}}(\mathbf{x}) = v_{\hat{k}, n}(\mathbf{x})e^{ip_f \hat{k}\cdot\mathbf{x}}.$$

The Andreev equations follow from BdG equations (7):

$$(\epsilon_{\hat{k}, n} + iv_f \hat{k}\boldsymbol{\nabla})u_{\hat{k}, n}(\mathbf{x}) = \Delta(\mathbf{x}, p_f \hat{k})v_{\hat{k}, n}(\mathbf{x})$$
$$(\epsilon_{\hat{k}, n} - iv_f \hat{k}\boldsymbol{\nabla})v_{\hat{k}, n}(\mathbf{x}) = \Delta^*(\mathbf{x}, p_f \hat{k})u_{\hat{k}, n}(\mathbf{x}) \qquad (28)$$

By approximating the domain wall profile with a step function, $\Delta(x, p_f \hat{k}) = \Delta\,\text{sgn}(x)\,g_{\hat{k}}$, the amplitudes for the zero-energy bound states are,

$$\begin{bmatrix} u_{\hat{k}, n} \\ v_{\hat{k}, n} \end{bmatrix}(\mathbf{x}) = \frac{1}{\sqrt{2}}\begin{bmatrix} 1 \\ -i\,\text{sgn}(\Delta_{\hat{k}f}^*) \end{bmatrix}\exp\left(-\left|\frac{\Delta g_{\hat{k}}\,x}{v_f \hat{k}_x}\right|\right) \qquad (29)$$

where Δ is the bulk amplitude of the order parameter, and $\Delta_{\hat{k}f} = \Delta\,\text{sgn}(\hat{k}_x)\,g_{\hat{k}}$ is the order parameter at the *final* end of the quasiclassical trajectory $\hat{k}$. Using this one finds that the coherence amplitudes between bound states at points $\hat{k}, \hat{k}'$ on the Fermi surface in the middle of the domain wall ($\mathbf{x} = -\mathbf{x}' = \mathbf{r}/2$) are

$$A_{\hat{k}\hat{k}'}^0(\mathbf{x})A_{\hat{k}\hat{k}'}^0(\mathbf{x}')^* = \left|\frac{1 + \text{sgn}(\Delta_{\hat{k}f}\Delta_{\hat{k}'f}^*)}{2}\right|^2$$
$$\times e^{-ip_f(\hat{k}-\hat{k}')\cdot\mathbf{r}}\,e^{-\frac{\Delta}{v_f}\left(\left|\frac{g_{\hat{k}}}{\hat{k}_x}\right| + \left|\frac{g_{\hat{k}'}}{\hat{k}_x'}\right|\right)|\mathbf{r}\hat{x}|} \qquad (30)$$

$$C_{\hat{k}\hat{k}'}^0(\mathbf{x})C_{\hat{k}\hat{k}'}^0(\mathbf{x}')^* = \left|\frac{1 - \text{sgn}(\Delta_{\hat{k}f}\Delta_{\hat{k}'f}^*)}{2}\right|^2$$
$$\times e^{ip_f(\hat{k}+\hat{k}')\cdot\mathbf{r}}\,e^{-\frac{\Delta}{v_f}\left(\left|\frac{g_{\hat{k}}}{\hat{k}_x}\right| + \left|\frac{g_{\hat{k}'}}{\hat{k}_x'}\right|\right)|\mathbf{r}\hat{x}|} \qquad (31)$$

The ordering vector $\mathbf{q} = p_f(\hat{k} - \hat{k}')$ that maximizes AA^* in (30) corresponds to combinations of $\hat{k}$ and $\hat{k}'$ that have same sign of $\Delta_{\hat{k}f}$ and $\Delta_{\hat{k}'f}$. For CC^* the ordering vector is $\mathbf{q} = p_f(\hat{k} + \hat{k}')$ and with replacement $\hat{k}' \to -\hat{k}'$ Eq. (31) results in the same relation between $\Delta_{\hat{k}f}$ and $\Delta_{\hat{k}'f}$. These vectors are illustrated in the bottom panel of figure 2.
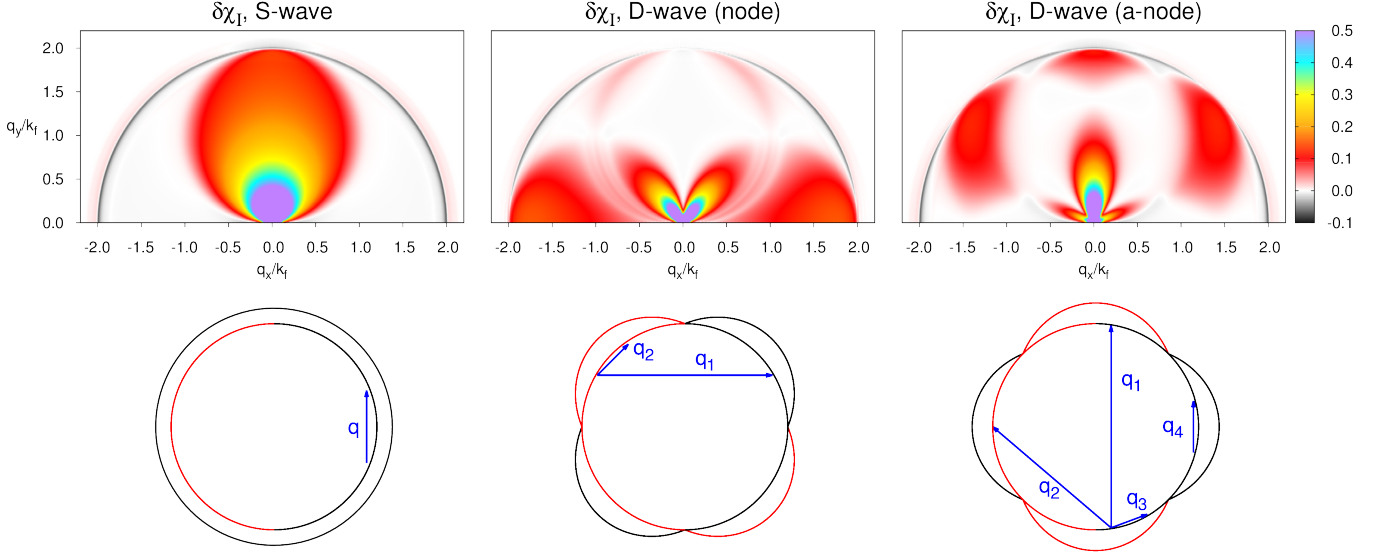
FIG. 2. Upper panels show static susceptibility $\delta\chi_I(0, \mathbf{q}, 0)$ as a function of ordering vector $\mathbf{q}$ at the center of the domain wall in the limit of low field $\mu_B H/\Delta_0 = 0.01$ and temperature $k_B T/\Delta_0 = 0.05$. The purple region around $\mathbf{q} = 0$ (uniform magnetization) has enhancement $\delta\chi_I' > 0.5$ due to large density of bound states and has been removed to better highlight the main features. The S-wave superconductor (left) favors $\mathbf{q}||\hat{y}$, along the domain wall. A domain wall along nodes of D-wave superconductor (middle) increases tendency for AFM with $q_x \sim 1.75 k_f$, across the domain wall. For antinodally-oriented domain wall (right) enhancement of χ shows for $\mathbf{q}/k_f \sim (0, 2)$ and $(1.25, 1)$. Bottom panels show ordering vectors $\mathbf{q}$ that connect points on the Fermi surface with same signs of $\Delta_{\hat{k}f}$ and $\Delta_{\hat{k}'f}$ that give largest coherence factors between zero-energy bound states. The OP at the final end of quasiclassical trajectory $\hat{k}$, $\Delta_{\hat{k}f}$, is a product of the domain wall spatial profile (inner circle) and the symmetry factor $g_{\hat{k}}$ (outer profile). black/red denote signs ± 1.

For S-wave $g_{\hat{k}} = 1$, and the two trajectories must end up on the same side of the domain wall, resulting in the $\mathbf{q}$ ordering generally along the domain wall. For D-wave, the two trajectories can be inside the same lobe on the same side of the domain wall giving small q_2 vectors, or there is a large wavevector $q_1 \lesssim 2k_f$ that connects points on the mirror lobes, corresponding to trajectories ending up on different sides of the domain wall.

Another slight enhancement for D-wave (node) can be seen as a circle of radius k_f centered at $(0, k_f)$, especially near wavevector $\mathbf{q}/k_f = (0.7, 1.7)$ and the ones obtained by symmetry operations. This enhancement cannot be explained by bound states, since for these wave vectors the amplitudes in (30-31) vanish. We suggest that these ordering vectors correspond to correlations between the bound states and the low-energy propagating states for near-nodal directions $|\Delta_{\hat{k}}| \lesssim \epsilon_\mathbf{n} \ll \Delta_0$. The free-propagating particle (p) and hole (h) type solutions $e^{\pm i k \hat{k} \cdot \mathbf{x}}$ are

$$\begin{bmatrix} u_{\hat{k},n} \\ v_{\hat{k},n} \end{bmatrix} \propto \begin{bmatrix} \epsilon + v_f k \\ \Delta_{\hat{k}}^* \end{bmatrix} e^{ik\hat{k}\cdot\mathbf{x}}, \begin{bmatrix} \Delta_{\hat{k}} \\ \epsilon + v_f k \end{bmatrix} e^{-ik\hat{k}\cdot\mathbf{x}} \quad (32)$$

with $v_f k = \sqrt{\epsilon^2 - |\Delta_{\hat{k}}|^2}$. Considering particle and hole scattering on the domain wall, we can find the exact wave functions of the propagating states along $\hat{k}$. For energies near the continuum edge, the eigenvectors are $\begin{bmatrix} u_{\hat{k},n}, & v_{\hat{k},n} \end{bmatrix} \propto \begin{bmatrix} 1, & \text{sgn}(\Delta_{\hat{k}}) \end{bmatrix}$ times appropriate reflec-

tion/transmission coefficients. The main feature of the propagating solutions is that they are real. Then combination of a bound state vector (29) for $\hat{k}$ with propagating state vector for $\hat{k}'$ results in

$$A_{\hat{k}\hat{k}'} A_{\hat{k}\hat{k}'}^* (0, \mathbf{r}) \propto e^{-ip_f(\hat{k}-\hat{k}')\cdot\mathbf{r}} e^{-\frac{\Delta}{v_f}\left(\left|\frac{g_{\hat{k}}}{\hat{k}_x}\right|\right)|\mathbf{r}\hat{x}|} \quad (33)$$

where dependence of the coherence factors on signs of the order parameter has disappeared, and similar for CC^*. Thus we have enhancement of susceptibility for vectors $\mathbf{q}$ that have tails at the bottom node of the gap and the heads tracing the bound states along the Fermi surface. We note, however, that such correlations at the domain wall are weighted by the particle/hole transmission and reflection coefficients, that can be small for $\epsilon \gtrsim |\Delta_{\hat{k}}|$.

In external field the energies of spin-up/down quasiparticles are shifted by $\pm\mu_B H$, and the zero-energy peak is split into two peaks, separated by energy $2\mu_B H$. This leads to reduction of $\Pi^\pm$ factors (21) and $\delta\chi_I$ shows very little enhancement over the normal state. In figure 3 we present $\delta\chi_I$ at the center of domain wall for applied field $\mu_B H = 0.4\Delta_0$, close to Pauli field, $\mu_B H_P \approx 0.7\Delta_0$ (S$-$wave), $0.55\Delta_0$(D$-$wave). At lower temperatures (panels B, D and F) the zero-field enhancement regions are still distinguishable but are much smaller, including the $q = 0$ uniform magnetization, since there is no zero-energy peak anymore. In D-wave (node) the enhancement at antiferromagnetic $q_x \sim 1.75 k_f$ is almost
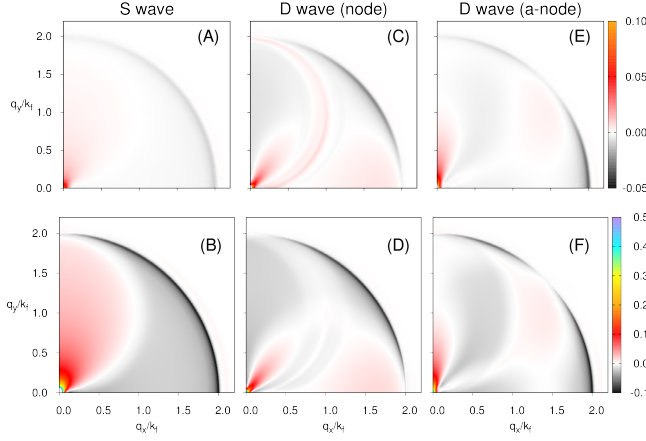
FIG. 3. Effects of magnetic field and temperature on $\delta\chi_I(\mathbf{q})$ at the center of domain wall. The zero-energy peaks are shifted by $\pm\mu_B H = \pm 0.4\Delta_0$, significantly reducing AFM correlations. Panels are for different temperatures: (A) $k_B T = 0.35\Delta_0$; (C,E) $k_B T = 0.2\Delta_0$; (B,D,F) $k_B T = 0.05\Delta_0$. Color scales to the right apply to the rows.

entirely wiped out. The higher temperature panels A, C and E reveal a further reduction of $\chi'(\mathbf{q})$ due to a smaller self-consistent gap and overall thermal smearing of the sum in (20). We note that higher fields and temperatures mostly reduce correlations involving bound states. This suppression of $\delta\chi_I$ with magnetic field at the domain wall is in stark contrast to behavior of susceptibility in the bulk, where magnetic field facilitates appearance of SDW correlations.[32–34]

B. Relaxation Rate

We also calculate the imaginary part of susceptibility taking $\omega \to 0$ (well-defined for unconventional superconductors only[35])

$$\chi''_\perp(\mathbf{x},\mathbf{x},\omega') \propto \sum_{\mathbf{nn'}\mu}$$

$$\Big[|A_{\mathbf{nn'}}(\mathbf{x})|^2[f(\epsilon_{\mathbf{n}\mu}) - f(\epsilon_{\mathbf{n'}\bar\mu})]\delta(\omega' + \epsilon_{\mathbf{n}\mu} - \epsilon_{\mathbf{n'}\bar\mu})$$

$$+ \frac{1}{2}|C_{\mathbf{nn'}}(\mathbf{x})|^2[f(\epsilon_{\mathbf{n}\mu}) - f(-\epsilon_{\mathbf{n'}\mu})]\delta(\omega' + \epsilon_{\mathbf{n}\mu} + \epsilon_{\mathbf{n'}\mu})$$

$$- \frac{1}{2}|C_{\mathbf{nn'}}(\mathbf{x})|^2[f(\epsilon_{\mathbf{n}\mu}) - f(-\epsilon_{\mathbf{n'}\mu})]\delta(\epsilon_{\mathbf{n}\mu} + \epsilon_{\mathbf{n'}\mu} - \omega')\Big]$$

to find the local spin-lattice relaxation rate (26) in static limit $T_1^{-1}(\mathbf{R} = \mathbf{x},\omega') = A_0^2 2T[\chi''_\perp(\mathbf{x},\mathbf{r} = 0,\omega')/\omega']_{\omega'\to 0}$:

$$\frac{1}{T_1(\mathbf{x})T} = -2A_0^2 \sum_{\mathbf{nn'}\mu} \frac{\partial f(\epsilon_{\mathbf{n}\mu})}{\partial\epsilon} \Big\{ |A_{\mathbf{nn'}}(\mathbf{x})|^2 \, \delta(\epsilon_{\mathbf{n}\mu} - \epsilon_{\mathbf{n'}\bar\mu})$$

$$+ |C_{\mathbf{nn'}}(\mathbf{x})|^2 \, \delta(\epsilon_{\mathbf{n}\mu} + \epsilon_{\mathbf{n'}\mu}) \Big\} . \quad (34)$$

where for numerical evaluation we use $\delta(\epsilon) = \omega''/\pi[\epsilon^2 + \omega''^2]$ with $\omega'' = 2.5 \times 10^{-3}\epsilon_f = \Delta_0/20$

The deviations of relaxation rate from the normal state's Korringa limit[36] are due to the spin-flip transitions between the low-energy states. Figures 4a and 4b provide numeric results for relaxation rate at the domain wall for S- and D-wave symmetry, with self-consistently determined bulk order parameter $\Delta(T, H)$. In S-wave one notices that the Hebel-Slichter coherence peak below T_c for $H \to 0$ is absent in the middle of the domain wall, due to *spatial* asymmetry of the order parameter. However, a peak develops for higher fields, but it lies not immediately below $T_c(H)$, but at lower temperatures. Similar enhancement of relaxation rate above the normal state's value can also be seen in D-wave. This peak appears due to transitions between the bound states and the continuum states, when $\epsilon_{\mathbf{k}\mu} \sim \Delta \pm \mu_B H = \mp\mu_B H = \epsilon_{0\bar\mu}$ ($\omega' \to 0$ limit), as schematically shown in figure 5.

For small fields in the static limit $2\mu_B H \approx \omega' \to 0$ the relaxation rate is divergent due to the sharp DOS of bound states, that should be compared to the logarithmic divergence in S-wave bulk superconductor associated with the sharpness of BCS coherence peaks.[30]

IV. CONCLUSIONS AND DISCUSSION

To summarize, we found that the concentration of zero-energy Andreev bound states (in zero field) at a domain wall defect in the order parameter leads to significant enhancement of the bare susceptibility. Since variations of the order parameter occur on scale of coherence length $\xi_c \gg 1/k_f$, the new quasiparticle environment inside the domain wall may lead to overall divergence of the total *local* susceptibility

$$\chi^{RPA}(\mathbf{R},\mathbf{q}) = \frac{\chi_\perp(\mathbf{R},\mathbf{q})}{1 - J_{\mathbf{q}}\,\chi_\perp(\mathbf{R},\mathbf{q})}$$

for antiferromagnetic ordering vector $\mathbf{q}$ ($q \sim k_f$), given sufficiently large exchange interaction $J_{\mathbf{q}}$. We find that the direction of the SDW modulation vector depends on the symmetry of the order parameter and orientation of its nodes relative to the domain wall. For S-wave gap, $\mathbf{q}$ is along the domain wall (i.e. $\mathbf{q} \perp \mathbf{q}_{FFLO}$), while for D-wave, when domain wall is aligned with its nodes, the $\mathbf{q}$-vector points across domain wall. The susceptibility enhancement is related to the increased correlations between bound states. These correlations disappear with magnetic field and temperature, something that was not seen in lattice models.

Our weak-coupling model does not support scenario of FFLO-induced magnetism in CeCoIn$_5$. First, the Q-phase appears in high magnetic fields[11,12] where we find bound state enhancement effects are wiped out. Moreover, even if the enhancement of susceptibility survives the field, from our calculation the direction of the SDW modulation is expected to be along the field (assuming $\mathbf{q}_{FFLO}||nodes||\mathbf{H}$), inconsistent with observations.[13] This, however, has to be checked further, since in our model we do not use the material-specific anisotropic

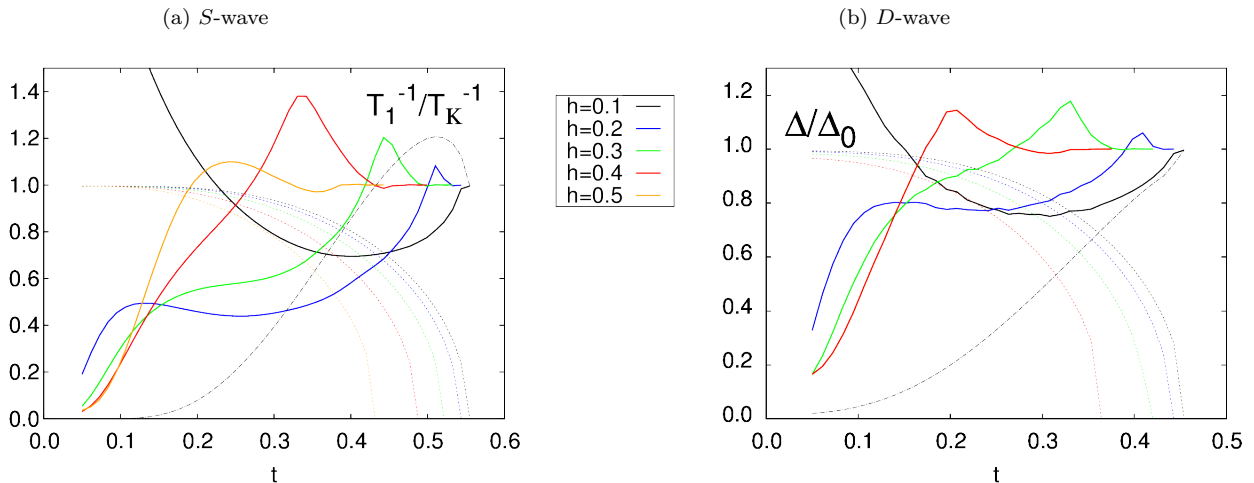(a) *S*-wave

(b) *D*-wave

FIG. 4. The relaxation rate at the center of domain wall, normalized to the Korringa limit, T_1^{-1}/T_K^{-1} (solid lines), and the bulk gap Δ/Δ_0 (dotted lines) as a function of temperature $t = k_B T/\Delta_0$ for different applied fields $h = \mu_B H/\Delta_0$. For higher fields, the enhancement of the relaxation rate above normal state value is due to transitions between bound states and the continuum states, when $\Delta(T, H) = 2\mu_B H$ (see Fig. 5), while at low fields the enhancement is due to transitions between bound states. This behavior is very different from that of the bulk relaxation rate (dot-dashed lines, shown for $h = 0.1$). In bulk *S*-wave one can see a Hebel-Schlicter peak that is suppressed for fields above $h \sim 0.15$.
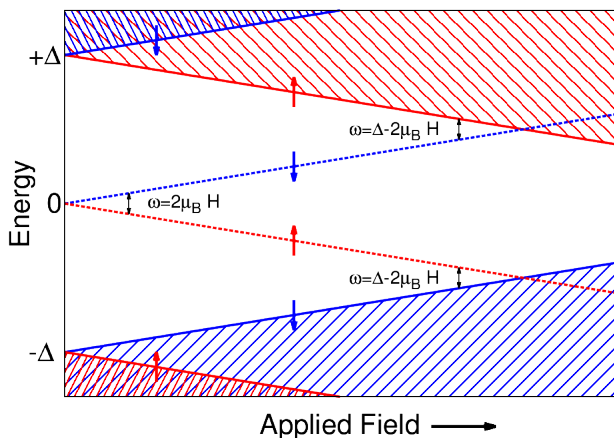

FIG. 5. Splitting of the energy states by Zeeman magnetic field. The bound states contribute to the relaxation rate T_1^{-1} at the domain wall either at small fields, where transitions between spin-flipped bound states are allowed, or at fields $2\mu_B H = \Delta$ that allow transitions between bound states and the low-lying continuum states at Δ.

Fermi surface. The nesting properties of the Fermi surface will be important for obtaining correct SDW vectors and instability conditions. On the other hand, some features of the high-field phase are rather more consistent with behavior of uniform state susceptibility,[33,34] and are independent of the exact shape of the Fermi surface. Direct comparison of our free-electron model with lattice models[18,19] is also difficult, for the same reason of having quite different input electronic energy dispersions. While both approaches give effective attraction between FFLO-type superconducting order and the antiferromagnetic order, the directions of emergent SDW vectors are not in complete alignment. Another difference between the these approaches could be related to the small size of the lattice grids, typically around 40×40 sites, which forces use of length scales $q_{FFLO} \sim 1/\xi_c \sim q \sim k_f$ (for comparison, we use $\xi_c k_f \sim 12$, and STM measurements[37,38] in CeCoIn$_5$ give $\xi_c \sim 60 \overset{\circ}{A}$, $k_f \sim (\pi/4.6)\overset{\circ}{A}^{-1}$ and $k_f \xi_c \approx 40$). This all calls for future more detailed investigation of emergent magnetic properties in nonuniform superconductors, that would clarify effects of the order parameter symmetry, spatial modulations, realistic Fermi surface anisotropy and field's orientation.

Finally, in nonuniform superconductor we find an increase of the spin-lattice relaxation rate T_1^{-1} over the Korringa limit. This enhancement mostly appears due to transitions between Andreev bound states and the propagating continuum states that can occur in high fields, $\mu_B H = 0.5\Delta$, close to the Pauli limiting field in *D*-wave $\mu_B H_P = 0.55\Delta_0$. The range of fields where it appears is in good agreement with experimental observations in κ-(BEDT-TTF)$_2$Cu(NCS)$_2$ near the first-order superconducting-normal transition,[14] although we find the magnitude of the enhancement is somewhat smaller than the measured value.

Appendix: Self-consistent order parameter

To calculate susceptibility $\chi(\mathbf{q}, \mathbf{R})$, which is a function of relative momentum $\mathbf{q}$, we choose a natural momentum-based Fourier expansion (10) to find self-consistent solutions of BdG amplitudes $u_\mathbf{n}(\mathbf{x}), v_\mathbf{n}(\mathbf{x})$ from (7) with order parameter (4). In the past, a variety of numeric or approximate methods have been used to address this problem: spatial lattice[19,39,40], Chebyshev polynomial expansion[41] or quasiclassical Greens functions.[15,28] Though effective, they are less suitable for our purpose.

The separable order parameter $\Delta(\mathbf{x}, \mathbf{x}') = \Delta(\mathbf{R})g(\mathbf{r})$ with relative $\mathbf{r} = \mathbf{x} - \mathbf{x}'$ and center-of-mass $\mathbf{R} = (\mathbf{x} + \mathbf{x}')/2$ coordinates is obtained from mean-field definition (4) using Bogoliubov transformation (5):

$$\Delta(\mathbf{R})\,g(\mathbf{r}) = V(\mathbf{r}) \sum_\mathbf{n}{}' \left\{ u_\mathbf{n}(\mathbf{x})v_\mathbf{n}^*(\mathbf{x}')\left[f(\epsilon_{\mathbf{n}\downarrow}) + f(\epsilon_{\mathbf{n}\uparrow})\right] \right.$$
$$\left. - u_\mathbf{n}(\mathbf{x}')v_\mathbf{n}^*(\mathbf{x})\left[f(-\epsilon_{\mathbf{n}\downarrow}) + f(-\epsilon_{\mathbf{n}\uparrow})\right]\right\}$$

(A.1)

where $f(\epsilon_{\mathbf{n}\mu}) = \langle\gamma_{\mathbf{n}\mu}^\dagger\gamma_{\mathbf{n}\mu}\rangle$ is the Fermi occupation number of state $\epsilon_{\mathbf{n}\mu}$ with spin μ. The prime on the sum denotes the cut-off restriction on the attractive potential $V(\mathbf{r})$, $|\epsilon_\mathbf{n}| < \Lambda$,[40] which for this report we set at $\Lambda = 5\Delta_0$, where $\Delta_0 = 0.05\epsilon_f$ is the zero temperature bulk order parameter. The amplitude of the order parameter is decomposed into CoM momentum Q (only x-component for the domain wall)

$$\Delta(R_x) = \int dQ\, \tilde{\Delta}(Q)\, e^{iQR_x}. \tag{A.2}$$

Using the Fourier expanded amplitudes (10) for momenta p along the domain wall, and $k = \{k_i\}$ in x direction, and introducing relative momentum, $\mathbf{r} \to \mathbf{q}$, we write the gap equation

$$\tilde{\Delta}(Q)\,g_{\hat{q}} = \sum_{\mathbf{n},p,k}{}' \tilde{u}_\mathbf{n}(k)\tilde{v}_\mathbf{n}^*(k-Q)$$
$$\left\{ \tilde{V}(\mathbf{q} - \mathbf{K})\left[f(\epsilon_{\mathbf{n}\downarrow}) + f(\epsilon_{\mathbf{n}\uparrow})\right]\right.$$
$$\left. - \tilde{V}(\mathbf{q} + \mathbf{K})\left[f(-\epsilon_{\mathbf{n}\downarrow}) + f(-\epsilon_{\mathbf{n}\uparrow})\right]\right\} \tag{A.3}$$

Here $\mathbf{K} = (k - Q/2)\hat{x} + p\hat{y}$, with magnitude $|\mathbf{K}|, |\mathbf{q}| \sim k_f$. We take separable interaction $\tilde{V}(\mathbf{q}-\mathbf{K}) = -V\,g_{\hat{q}}\,g_{\hat{K}}^*$ with a constant V. Then

$$\tilde{\Delta}(Q) = V\sum_{\mathbf{n},p,k,\mu}{}' \tilde{u}_\mathbf{n}(k)\tilde{v}_\mathbf{n}^*(k-Q)g_{\hat{K}}\tanh\left[\frac{\epsilon_{\mathbf{n}\mu}}{2T}\right] \tag{A.4}$$

The interaction parameter V is eliminated together with the cut-off Λ using the zero temperature and field value Δ_0. We recursively solve (14) with (A.4) until sufficient convergence for profile $\Delta(R_x)$ is reached.

---

[1] J. Bardeen, L. N. Cooper, and J. R. Schrieffer, Phys. Rev. **108**, 1175 (1957).

[2] P. Fulde and R. A. Ferrell, Phys. Rev. **135**, A550 (1964).

[3] A. Larkin and I. Ovchinnikov, Soviet Physics-JETP **20**, 762 (1965).

[4] C.-R. Hu, Phys. Rev. Lett. **72**, 1526 (1994).

[5] C. Caroli, P. D. Gennes, and J. Matricon, Physics Letters **9**, 307 (1964), ISSN 0031-9163.

[6] M. Eschrig, Reports on Progress in Physics **78**, 104501 (2015).

[7] Y. Tanaka, M. Sato, and N. Nagaosa, Journal Of The Physical Society Of Japan **81**, 011013 (2012).

[8] T. Mizushima, Y. Tsutsumi, T. Kawakami, M. Sato, M. Ichioka, and K. Machida, Journal of the Physical Society of Japan **85**, 022001 (2016).

[9] Y. Nagato, S. Higashitani, and K. Nagai, Journal of the Physical Society of Japan **78**, 123603 (2009).

[10] S. B. Chung and S.-C. Zhang, Phys. Rev. Lett. **103**, 235301 (2009).

[11] M. Kenzelmann, T. Strssle, C. Niedermayer, M. Sigrist, B. Padmanabhan, M. Zolliker, A. D. Bianchi, R. Movshovich, E. D. Bauer, J. L. Sarrao, et al., Science **321**, 1652 (2008).

[12] M. Kenzelmann, S. Gerber, N. Egetenmeyer, J. L. Gavilano, T. Strässle, A. D. Bianchi, E. Ressouche, R. Movshovich, E. D. Bauer, J. L. Sarrao, et al., Phys. Rev. Lett. **104**, 127001 (2010).

[13] S. Gerber, M. Bartkowiak, J. L. Gavilano, E. Ressouche, N. Egetenmeyer, C. Niedermayer, A. D. Bianchi, R. Movshovich, E. D. Bauer, J. D. Thompson, et al., Nature Physics **10**, 126 (2014).

[14] H. Mayaffre, S. Kramer, M. Horvatic, C. Berthier, K. Miyagawa, K. Kanoda, and V. F. Mitrovic, Nat Phys **10**, 928 (2014), ISSN 1745-2473.

[15] H. Burkhardt and D. Rainer, Annalen der Physik **506**, 181 (1994), ISSN 1521-3889.

[16] A. B. Vorontsov and M. J. Graf, J. Low Temp. Phys. pp. 729–730 (2006).

[17] Y. Yanase and M. Sigrist, Journal of the Physical Society of Japan **78**, 114715 (2009).

[18] Y. Yanase and M. Sigrist, Journal of Physics: Conference Series **150**, 052287 (2009).

[19] M. Mierzejewski, A. Ptok, and M. M. Maśka, Phys. Rev. B **80**, 174525 (2009).

[20] Y. Yanase and M. Sigrist, Journal of Physics: Condensed Matter **23**, 094219 (2011).

[21] M. Takigawa, M. Ichioka, and K. Machida, Phys. Rev. Lett. **83**, 3057 (1999).

[22] Y. Nakai, Y. Hayashi, K. Ishida, H. Sugawara, D. Kikuchi, and H. Sato, Physica B: Condensed Matter **403**, 1109 (2008), ISSN 0921-4526, proceedings of the International Conference on Strongly Correlated Electron Systems.

[23] K. K. Tanaka, M. Ichioka, S. Onari, N. Nakai, and K. Machida, Phys. Rev. B **91**, 014509 (2015).

[24] K. M. Suzuki, M. Ichioka, and K. Machida, Phys. Rev. B **83**, 140503 (2011).

[25] M. OGATA, International Journal of Modern Physics B **13**, 3560 (1999).

[26] J.-X. Zhu and C. S. Ting, Phys. Rev. Lett. **87**, 147002 (2001).

[27] A. Ghosal, C. Kallin, and A. J. Berlinsky, Phys. Rev. B **66**, 214502 (2002).

[28] A. B. Vorontsov, J. A. Sauls, and M. J. Graf, Phys. Rev. B **72**, 184501 (2005).

[29] R. Kubo, Journal of the Physical Society of Japan **12**, 570 (1957).

[30] M. Tinkham, *Introduction to Superconductivity* (McGraw-Hill, 1996), 2nd ed.

[31] A. Abragam, *The Principles of Nuclear Magnetism* (Oxford, 1962).

[32] R. Ikeda, Y. Hatakeyama, and K. Aoyama, Physical Review B **82**, 060510 (2010).

[33] Y. Kato, C. D. Batista, and I. Vekhter, Phys. Rev. Lett. **107**, 096401 (2011).

[34] B. M. Rosemeyer and A. B. Vorontsov, Phys. Rev. B **89**, 220501 (2014).

[35] M. Sigrist and K. Ueda, Rev. Mod. Phys. **63**, 239 (1991).

[36] J. Korringa, Physica **16**, 601 (1950), ISSN 0031-8914.

[37] B. B. Zhou, S. Misra, E. H. d. S. Neto, P. Aynajian, R. E. Baumbach, J. D. Thompson, E. D. Bauer, and A. Yazdani, Nature Physics **9**, 474 (2013).

[38] M. P. Allan, F. Massee, D. K. Morr, J. V. Dyke, A. W. Rost, A. P. Mackenzie, C. Petrovic, and J. C. Davis, Nature Physics **9**, 468 (2013).

[39] A. M. Martin and J. F. Annett, Phys. Rev. B **57**, 8709 (1998).

[40] M. Franz and Z. Tešanović, Phys. Rev. Lett. **80**, 4763 (1998).

[41] L. Covaci, F. M. Peeters, and M. Berciu, Phys. Rev. Lett. **105**, 167006 (2010).